

sense of  $J$  and  $J/z$  becomes indefinite upon the increase of the  $J/z/J$  ratio because the equation used for the fitting is developed under assumption that  $J \gg J/z$ . It is especially important in the case of  $\text{Cu}_2(\text{hfac})_3(\text{EtL})_2$ , where this ratio exceeds 0.1.

### Conclusions

The reaction of  $\text{Cu}(\text{hfac})_2$  with sterically hindered 3-imidazoline hydroxylamines in inert atmosphere yields new types of mixed-ligand complexes with nitroxides of the composition  $\text{Cu}_2(\text{hfac})_3(\text{RL})_2$ , which are not formed on the direct reaction of  $\text{Cu}(\text{hfac})_2$  with RL. The polymeric structure of  $\text{Cu}_2(\text{hfac})_3(\text{EtL})_2$  in solid phase has been determined, this structure being characterized by the  $\text{Cu}^+$  and  $\text{Cu}^{2+}$  ion alternation in the chain manner and also by the coordination of two N+O fragments to  $\text{Cu}^{2+}$  ions. In N+O— $\text{Cu}^{2+}$ —O+N exchange clusters existing in solid  $\text{Cu}_2(\text{hfac})_3(\text{RL})_2$ , ferromagnetic exchange interactions are realized.

In the course of the investigation  $[\text{Cu}(\text{hfac})_2]_3(\text{EtL})_2$  and  $[\text{Cu}(\text{hfac})_2]_3(i\text{-PrL})_2$  were obtained as well, which are representatives of the recently discovered type of mixed-ligand complex

with nitroxides.<sup>14,23</sup> The structure and magnetic properties of these compounds are the subject of further investigation and will be reported later.

**Acknowledgment.** We thank Dr. P. P. Semyannikov for recording the mass spectra.

**Registry No.**  $\text{Cu}_2(\text{hfac})_3(\text{PhL})_2$ , 131729-29-8;  $\text{Cu}(\text{hfac})_2$ , 14781-45-4;  $\text{Cu}_2(\text{hfac})_3(\text{EtL})_2$ , 131729-30-1;  $\text{Cu}_2(\text{hfac})_3(i\text{-PrL})_2$ , 131729-31-2;  $\text{Cu}(\text{hfac})_2(\text{MeLH})$ , 120660-34-6;  $\text{Cu}(\text{hfac})_2(i\text{-PrLH})$ , 131758-59-3;  $\text{Cu}(\text{hfac})_2(\text{PhLH})$ , 131729-32-3;  $[\text{Cu}(\text{hfac})_2]_3(\text{EtL})_2$ , 126913-32-4;  $[\text{Cu}(\text{hfac})_2]_3(i\text{-PrL})_2$ , 126942-92-5;  $\text{Cu}(\text{hfac})(\text{MeLH})_2$ , 131758-60-6;  $\text{Cu}_2(\text{hfac})_3(\text{MeL})_2$ , 113677-67-1.

**Supplementary Material Available:** Tables 1-4, listing C, H, N, and Cu analytical data, bond lengths and angles, anisotropic thermal parameter coefficients, and root-mean-square planes (8 pages); Table 5, listing structure factors (41 pages). Ordering information is given on any current masthead page.

(23) Caneschi, A.; Gatteschi, D.; Sessoli, R.; Hoffman, S. K.; Laugier, J.; Rey, P. *Inorg. Chem.* 1988, 27, 2390-2392.

Contribution from the Laboratoire de Chimie des Métaux de Transition, Unité de Recherche Associée au CNRS No. 419, Université Pierre et Marie Curie, 75252 Paris Cedex 05, France, and Department of Chemistry, Georgetown University, Washington, D.C. 20057-0001

## Disubstituted Tungstosilicates. 2. $\gamma$ - and $\beta$ -Isomers of $[\text{SiV}_2\text{W}_{10}\text{O}_{40}]^{6-}$ : Syntheses and Structure Determinations by $^{183}\text{W}$ , $^{51}\text{V}$ , and $^{29}\text{Si}$ NMR Spectroscopy

Jacqueline Canny,<sup>†</sup> René Thouvenot,<sup>†</sup> André Tézé,<sup>†</sup> Gilbert Hervé,<sup>\*†</sup> Michele Leparulo-Loftus,<sup>‡</sup> and Michael T. Pope<sup>†</sup>

Received March 23, 1990

Addition of vanadium to the divacant  $\gamma$ - $[\text{HSiW}_{10}\text{O}_{36}]^{7-}$  anion gives quantitatively the  $\gamma$ -decatungsto-1,2-divanadosilicate  $[\text{SiV}_2\text{W}_{10}\text{O}_{40}]^{6-}$  parent complex. This complex is stable in nonaqueous solution but isomerizes in water. The isomerization was followed by polarography, and depending on the experimental conditions, three geometrical isomers of  $[\text{SiV}_2\text{W}_{10}\text{O}_{40}]^{6-}$  were prepared (as pure compounds for two of them). These isomers are characterized by their IR spectra and their  $^{183}\text{W}$ ,  $^{51}\text{V}$ , and  $^{29}\text{Si}$  NMR spectra. All have the  $\beta$ -structure with the two vanadium atoms in positions (8,12), (3,12), and (3,8), respectively.

### Introduction

The synthesis of polyoxotungstates or molybdates of the Keggin structure in which W or Mo atoms are partially replaced by atoms such as  $\text{Ti}^{\text{IV}}$ ,  $\text{Nb}^{\text{V}}$ , or  $\text{V}^{\text{V}}$  has attracted increasing attention because of (i) the use of these compounds in oxidation catalysis<sup>1</sup> and (ii) the use of the compounds to link organometallic moieties on the surface oxygen atoms.<sup>2</sup> Important changes of the solution or solid-state properties of these compounds, such as the redox behavior and the strength of the acid, can be expected when the number (usually 1, 2, or 3) and the vicinity of these addenda atoms in the Keggin structure are modified.

A better knowledge of the factors that influence the relative positions of the addenda atoms is required in order to rationalize stereospecific methods for synthesizing such compounds. A possible approach of this problem consists of the preparation of a pure and well-characterized derivative and the study of its isomerization under various conditions (solvent, acidity, temperature, etc.).

This paper deals with the preparation of the divanadium derivative of the  $\gamma$ -12-tungstosilicate obtained from the divacant  $\gamma$ - $[\text{HSiW}_{10}\text{O}_{36}]^{7-}$  polyanion and its isomerization into three different geometric isomers according to the experimental conditions. Let us be reminded that  $\beta$ - and  $\gamma$ -isomers of the Keggin anion ( $\alpha$ -isomer) are derived from the latter by rotation of one or two groups of three edge-sharing  $\text{WO}_6$  octahedra, respectively (Figure 1).<sup>3</sup> All the divanadium compounds have been characterized by

polarography,  $^{29}\text{Si}$ ,  $^{51}\text{V}$ , and  $^{183}\text{W}$  NMR spectroscopy in solution, and infrared spectroscopy in the solid state. A preliminary report of this work has been presented.<sup>4</sup>

### Experimental Section

**Preparation of Compounds.** **Ia**,  $\text{Cs}_4\text{H}_2\text{-}\gamma(1,2)\text{-}[\text{SiV}_2\text{W}_{10}\text{O}_{40}]\text{4H}_2\text{O}$ .<sup>5</sup> This compound was prepared by using the potassium salt of the  $\gamma$ -10-tungstosilicate obtained as previously described.<sup>6</sup> This salt (10 g,  $3.33 \times 10^{-3}$  mol) is dissolved in 1 M HCl (35 mL), 0.5 M sodium metavanadate ( $\text{NaVO}_3$ ) (13.5 mL,  $6.75 \times 10^{-3}$  mol) is added, and the mixture is gently stirred a few minutes. A small precipitate is filtered off (solution A). Cesium chloride (5 g) is added to the clear solution. The solid is separated by filtration on a fine frit. This crude product is dissolved in 0.5 M HCl (400 mL), and small quantities of insoluble material are

- (1) For a review, see: Misono, M. *Catal. Rev.—Sci. Eng.* 1987, 269 and references therein.
- (2) Among the abundant literature see the following: (a) For niobium-substituted polyanions: Edlund, D. J.; Saxton, R. J.; Lyon, D. K.; Finke, R. G. *Organometallics* 1988, 7, 1692. Finke, R. G.; Droege, M. W. *J. Am. Chem. Soc.* 1984, 106, 7274. Day, V. W.; Klemperer, W. G.; Maltby, D. J. *Organometallics* 1985, 4, 104. (b) For vanadium-substituted polyanions: Finke, R. G.; Rapko, B.; Saxton, R. J.; Domaille, P. J. *J. Am. Chem. Soc.* 1986, 108, 2947.
- (3) Baker, L. C. W.; Figgis, J. S. *J. Am. Chem. Soc.* 1970, 92, 3794. Pope, M. T. *Isopoly and Heteropoly Oxometalate Anions*; Springer-Verlag: Berlin, 1983; p 26.
- (4) Tézé, A.; Canny, J.; Leyrie, M.; Hervé, G. Presented at the CNRS-NSF Workshop on Polyoxometalates, Saint-Lambert des Bois, France, 1983.
- (5) (a) Dodecaoxometalate  $[\text{SiV}_2\text{W}_{10}\text{O}_{40}]^{6-}$  isomers will be abbreviated by the trivial notation used in the literature of  $\alpha$ ,  $\beta$ , or  $\gamma$ , followed by the number of the vanadium positions according to the IUPAC recommendations (in parentheses). (b) Jeannin, Y.; Fournier, M. *Pure Appl. Chem.* 1987, 59, 1529.
- (6) Canny, J.; Tézé, A.; Thouvenot, R.; Hervé, G. *Inorg. Chem.* 1986, 25, 2114.

<sup>†</sup> Université Pierre et Marie Curie.

<sup>‡</sup> Georgetown University.

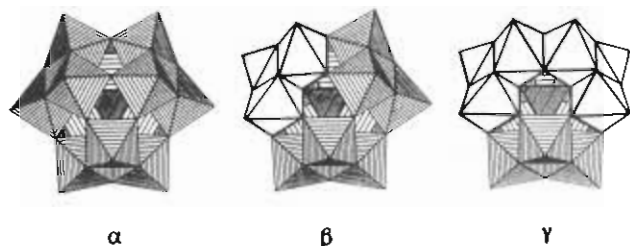


**Figure 1.** Polyhedral representation of the Keggin anion  $\alpha$ -[SiW<sub>12</sub>O<sub>40</sub>]<sup>4-</sup> and of its  $\beta$ - and  $\gamma$ -isomers. The rotated groups of three edge-sharing WO<sub>6</sub> octahedra are represented in white in the structures of the  $\beta$ - and  $\gamma$ -anions.

eliminated. The desired salt is precipitated again by addition of CsCl (10 g), filtered, and air-dried (yield: 10 g).

Anal. Calcd for Cs<sub>4</sub>H<sub>2</sub>[SiV<sub>2</sub>W<sub>10</sub>O<sub>40</sub>]-4H<sub>2</sub>O: Cs, 16.5; Si, 0.87; W, 57.2; V, 3.2; H<sub>2</sub>O, 2.2. Found: Cs, 16.6; Si, 0.95; W, 54.1; V, 2.9; H<sub>2</sub>O, 2.2.

**Ib, H<sub>6</sub>- $\gamma$ (1,2)-[SiV<sub>2</sub>W<sub>10</sub>O<sub>40</sub>].** Solution A, obtained as described in the preparation of compound **Ia**, is transferred into a 250-mL separatory funnel. The acid is extracted by addition of 20 mL of diethyl ether and 50 mL of a mixture of an equal volume of diethyl ether and 12 M HCl chilled to -20 °C. The heavier layer is collected, and diethyl ether is removed under vacuum. The acid **Ib** is obtained as a fine pale yellow powder.

**IIa, Cs<sub>6</sub>- $\beta$ (8,12)-[SiV<sub>2</sub>W<sub>10</sub>O<sub>40</sub>]-9H<sub>2</sub>O.** Solution A is brought to pH 6.5–6.8 with sodium hydroxide. The pH of the solution is maintained at this value for 4 h by addition of small portions of 1 M HCl. The desired salt is obtained by addition of solid CsCl (7 g) to the orange-red solution (solution B) and filtered (yield: 10 g).

Anal. Calcd for Cs<sub>6</sub>[SiV<sub>2</sub>W<sub>10</sub>O<sub>40</sub>]-9H<sub>2</sub>O: Cs, 22.3; Si, 0.79; W, 51.5; V, 2.85; H<sub>2</sub>O, 4.5. Found: Cs, 21.8; Si, 0.80; W, 51.6; V, 2.9; H<sub>2</sub>O, 4.6.

**IIb, H<sub>6</sub>- $\beta$ (8,12)-[SiV<sub>2</sub>W<sub>10</sub>O<sub>40</sub>].** Solution B, obtained as described for the preparation of compound **IIa**, is transferred into a 250-mL separatory funnel. The acid is extracted by addition of 20 mL of diethyl ether and 10 mL of a mixture of equal volumes of diethyl ether and sulfuric acid chilled to -20 °C. The heavier layer is collected and diethyl ether removed under vacuum. The acid **IIb** is obtained as a fine red-orange powder.

**IIIa, Cs<sub>6</sub>- $\beta$ (3,8)-[SiV<sub>2</sub>W<sub>10</sub>O<sub>40</sub>]-12H<sub>2</sub>O.** Solution A is brought to pH 8.15 with sodium hydroxide. The pH of the solution is maintained between 8.0 and 8.3 by addition of small portions of 1 M HCl. The reaction is stopped when the pH does not significantly change over a period of 10 min (total time: 3–4 h). The fine precipitate that appears at the end of the transformation is filtered off on a sintered-glass filter. The desired product is obtained by addition of solid CsCl (7 g) to the orange-red solution. It is dissolved in water (1100 mL). A small quantity of insoluble material is filtered off. The complex is precipitated again by addition of CsCl (20 g) (yield: 9 g).

Anal. Calcd for Cs<sub>6</sub>[SiV<sub>2</sub>W<sub>10</sub>O<sub>40</sub>]-12H<sub>2</sub>O: Cs, 22.0; Si, 0.78; W, 50.8; V, 2.8; H<sub>2</sub>O, 6.0. Found: Cs, 22.3; Si, 0.76; W, 49.7; V, 2.8; H<sub>2</sub>O, 5.8.

**IVb, H<sub>6</sub>- $\beta$ (3,12)-[SiV<sub>2</sub>W<sub>10</sub>O<sub>40</sub>].** The acid of the  $\gamma$ -isomer (compound **Ib**, 10 g) is dissolved in 10 mL of water, and this solution is kept at room temperature for 5 weeks and then transferred into a 100-mL separatory funnel. Diethyl ether (15 mL) and, slowly, 8 M sulfuric acid (2 mL) were added. A yellow heavier layer is eliminated, and sulfuric acid (3 mL) is then added. The red heavier layer is collected, and diethyl ether is removed under vacuum. The fine red-orange powder obtained is a mixture of the  $\beta$ (8,12) and  $\beta$ (3,12) acids.

**NMR Spectra.** The <sup>29</sup>Si, <sup>51</sup>V and <sup>183</sup>W NMR spectra were recorded in 10-mm-o.d. tubes on WM 250 (<sup>29</sup>Si, <sup>51</sup>V and <sup>183</sup>W) and on WM 500 (<sup>183</sup>W) Bruker instruments, both operating in the Fourier mode at 49.6 MHz (<sup>29</sup>Si), 65.7 MHz (<sup>51</sup>V), and 10.4 and 20.8 MHz (<sup>183</sup>W), respectively. Chemical shifts are referenced with respect to external neat TMS and VOCl<sub>3</sub> and alkaline aqueous WO<sub>4</sub><sup>2-</sup> respectively, with negative values upfield of the standard. For the <sup>51</sup>V NMR spectroscopy, chemical shifts were measured with respect to external alkaline aqueous VO<sub>4</sub><sup>3-</sup> used as a secondary standard.

Concentrated aqueous solutions required for the poorly receptive <sup>183</sup>W nucleus were prepared by dissolving the polyanion, as the poorly soluble cesium salt, in a saturated aqueous LiClO<sub>4</sub> solution and filtering off the cesium perchlorate precipitate. The perchlorate excess in solution does not affect the NMR characteristics of the spectrum. This procedure, as compared with a resin-exchange procedure, offers two essential advantages: it is very quick to perform, and very concentrated solutions are directly obtained without the need of further manipulations eventually damaging to unstable species.

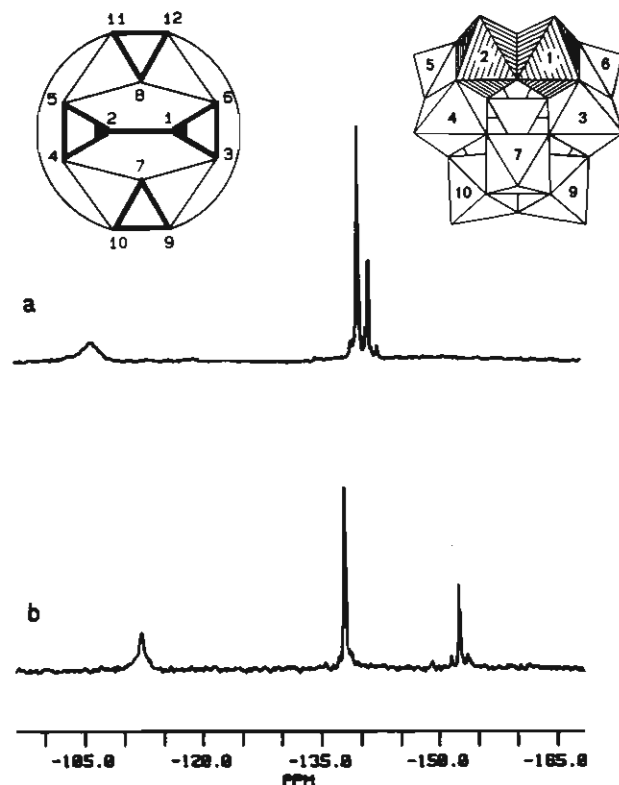


**Figure 2.** 10.4-MHz <sup>183</sup>W NMR spectra of the  $\gamma$ (1,2)-[SiV<sub>2</sub>W<sub>10</sub>O<sub>40</sub>]<sup>6-</sup> anion: (a, upper part) acidic form at pH < 0, 11 400 scans; (b, lower part) deprotonated anion at pH 3, 8020 scans. The schematic plane representation and atom numbering are in accordance with the IUPAC recommendations. Heavy and thin lines symbolize edge- and corner-sharing junctions respectively. The vanadium positions are depicted by black triangles in the flat representation and by hatched octahedra in the polyhedra representation. Dodecaoxometalate [SiV<sub>2</sub>W<sub>10</sub>O<sub>40</sub>]<sup>6-</sup> isomers are abbreviated by the trivial notation used in the literature of  $\alpha$ ,  $\beta$ , or  $\gamma$ , followed by the number of the vanadium positions according to the IUPAC recommendations (in parentheses).

The IR spectra were recorded on a Perkin-Elmer 283 scanning spectrometer (4000–200-cm<sup>-1</sup> range) as KBr pellets.

The polarograms were recorded in a 1 M acetic acid–1 M sodium acetate buffer. All the potential values were referred to the saturated calomel electrode.

## Results and Discussion

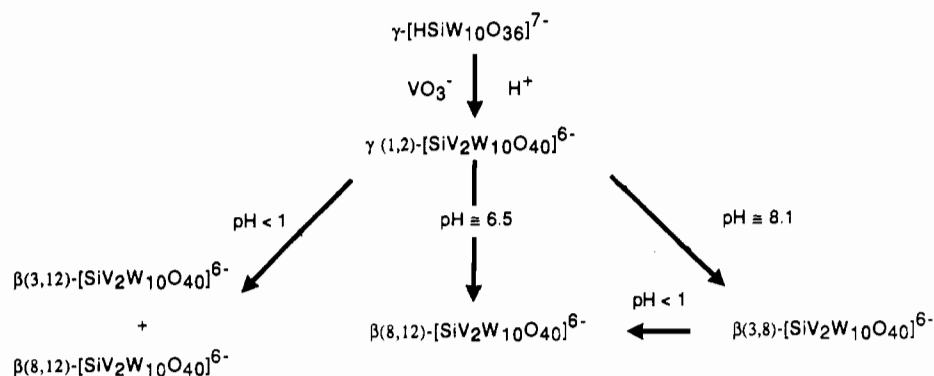
**The  $\gamma$ (1,2)-[SiV<sub>2</sub>W<sub>10</sub>O<sub>40</sub>]<sup>6-</sup> Polyanion.** The addition of a stoichiometric amount of vanadate in the solution of  $\gamma$ -[HSiW<sub>10</sub>O<sub>36</sub>]<sup>7-</sup> gives quantitatively the yellow dinuclear complex [SiV<sub>2</sub>W<sub>10</sub>O<sub>40</sub>]<sup>6-</sup> (**I**) at pH 5 or its diprotonated form [H<sub>2</sub>SiV<sub>2</sub>W<sub>10</sub>O<sub>40</sub>]<sup>4-</sup> in acid solution (pH < 1).

The structure of  $\gamma$ -[HSiW<sub>10</sub>O<sub>36</sub>]<sup>7-</sup> is retained in the complex as shown by comparison of the <sup>183</sup>W NMR spectra of the initial polyanion<sup>6</sup> and of the complex (Figure 2): three resonance lines, in nearly 2:2:1 relative intensities, were observed in both spectra. In the  $\gamma$ -[HSiW<sub>10</sub>O<sub>36</sub>]<sup>7-</sup> ligand, the resonance lines have been previously assigned to the different tungsten atoms.<sup>6</sup>

From previous studies on vanadium-substituted polytungstates,<sup>7</sup> the assignment of peaks is based on the following assumptions. Two kinds of tungsten atoms are expected according to the vanadium atom proximity: the resonance lines of tungsten atoms only two bonds removed from vanadium are relatively broad with respect to resonance lines of other tungstens further removed from the substitution site. This broadening, originating from a partial coalescence of the tungsten–vanadium octuplet, depends on the quadrupolar relaxation of the vanadium nucleus and on the <sup>2</sup>J<sub>W-V</sub> coupling constant. It is evident that variations of these parameters can lead to more or less broadened lines (between 5 and 100 Hz), but these lines will be always distinguishable from the sharp lines

(7) Domaille, P. J. *J. Am. Chem. Soc.* 1984, 106, 7677.

Scheme I



(about 1 Hz). Moreover, according to Domaille,<sup>7</sup> tungsten atoms only edge shared to vanadium ones are expected to give relatively sharp lines (half-width less than 20 Hz) with respect to tungsten atoms corner shared to vanadium ones. In fact, Domaille's observed and simulated spectra clearly demonstrate that, irrespective of the temperature, the lines are always about three times broader for corner- than for edge-coupled tungsten nuclei. In the case of vanadium disubstituted polyoxotungstates, additional broadening is expected for tungsten atoms coupled to two vanadium nuclei, with the highest effect when both are corner coupled.

The high-frequency broad line (-112 ppm) observed with the nonprotonated  $\gamma\text{-[SiV}_2\text{W}_{10}\text{O}_{40}]^{6-}$  polyanion (Figure 2b) is assigned to the four W(3), W(4), W(5), and W(6) equivalent atoms adjacent to the vanadium atoms. The two other (sharp) lines are assigned according to their multiplicity: that at -138 ppm to the four equivalent W(9), W(10), W(11), and W(12) atoms and that at -152 ppm to the two equivalent W(7) and W(8) atoms. The corner tungsten-tungsten coupling between both atoms with a four multiplicity (W(3), W(9), and equivalent pairs) is 16 Hz, but it was only 5 Hz in the divacant  $\gamma\text{-[HSiW}_{10}\text{O}_{36}]^{7-}$  polyanion.<sup>6</sup> That means that a reequilibrium of all interatomic distances and angles rendering the anion like a saturated unsubstituted Keggin anion occurs upon the complex formation. This complex shows a single <sup>51</sup>V NMR line (-555.9 ppm,  $\Delta\nu_{1/2} = 650$  Hz, pH 3).

In acid solution, the protonation of the anion results in some interesting effects (Figure 2a). Due to the high anion concentration, pH measurements are not very precise; therefore, the NMR/acidity correlation is only qualitative. A substantial broadening of the low-field <sup>183</sup>W resonance line from about 5 to about 20 Hz is observed. According to the theory developed by Domaille,<sup>7</sup> it could be interpreted by a strengthening of the vanadium-tungsten coupling constants and/or an alteration of the relaxation properties of the vanadium atoms. In fact, the single <sup>51</sup>V resonance line sharpens and shifts significantly on protonation: from 650 Hz at -555.9 ppm for the deprotonated anion to 190 Hz at -587 ppm for the protonated one. For the deprotonated anion, the very short relaxation time (less than 1 ms) of the vanadium atom allows an effective self-decoupling of the nearby tungsten atoms. Moreover, the tungsten-tungsten coupling constant between W(3) and W(9) increases from 16 to 19 Hz on protonation.

The complex is easily characterized in solution by polarography on the dropping mercury electrode in a 1 M acetic acid-1 M sodium acetate buffer. After the ill-defined waves due to the reduction of the vanadium atoms ( $\text{V}^{\text{V}}/\text{V}^{\text{IV}}$  and  $\text{V}^{\text{IV}}/\text{V}^{\text{III}}$ ), two 2-electron waves corresponding to the reduction of tungsten atoms characterize the  $\gamma\text{-[SiW}_{10}\text{O}_{36}]$  framework. The half-wave potentials for the complex (-0.70 and -0.83 V) are slightly less negative than the  $E_{1/2}$  of the corresponding waves for the free ligand under the same conditions (-0.74 and -0.85 V). These differences can be understood if we consider the global charge of the polyanion.<sup>8</sup> When the reduction of the tungsten atoms

occurs, the charge of  $\gamma\text{-[SiV}_2\text{W}_{10}\text{O}_{38}(\text{H}_2\text{O})_2]^{6-}$  is smaller than that of  $\gamma\text{-[HSiW}_{10}\text{O}_{36}]^{7-}$ , and hence reduction of the complex is slightly easier.

A structure of the complex in which the vanadium atoms occupy the two adjacent vacant sites of the defect  $\gamma\text{-[HSiW}_{10}\text{O}_{36}]^{7-}$  polyanion<sup>6</sup> agrees with all these results. The essential structural feature of the complex is the bis( $\mu$ -oxo) bridge between the vanadium atoms. This species is isostructural with the  $\gamma\text{-[PV}_2\text{W}_{10}\text{O}_{40}]^{5-}$  polyanion previously described.<sup>9</sup>

**Stability and Isomerization of  $\gamma(1,2)\text{-[SiV}_2\text{W}_{10}\text{O}_{40}]^{6-}$ .** The vanadium complex can be dissolved in organic solvents such as acetonitrile as tetrabutylammonium salt. The solution was unchanged after overnight boiling. On the contrary, the aqueous solution is not stable whatever the conditions. Between pH 3 and 5, the evolution of I is very slow. Outside this pH range, pH-dependent isomerization reactions occur. These are easily monitored by polarography in acetic buffer because, once formed, all the products are stable in this medium and present well-defined characteristic tungsten reduction waves at a dropping mercury electrode.

At pH 6-7, the decrease of the waves due to the  $\gamma$ -isomer (-0.70 and -0.83 V) and the increase of the height of new waves at -0.75 and -0.89 V have been observed at room temperature. The transformation was almost complete after 2 h. The new polyanion (II) has been isolated as a cesium salt or as an acid. It is stable in aqueous solution even while the solution is boiling, at pH < 8.5. Analyses showed that II had the same composition as the initial  $\gamma$ -complex, and it will be shown later to be the  $\beta(8,12)$ -isomer.

At pH 8-9, the solution of the  $\gamma$ -complex evolved more rapidly into another anion (III) characterized by two-electron tungsten reduction waves at -0.82 and -1.03 V in acetic buffer. It has been obtained as the Cs<sup>+</sup> salt. Analyses showed that III is also an isomer of I and II anions, and it will be shown later to be the  $\beta(3,8)$ -isomer. When a solution of II was maintained at pH 8-9, it did not transform into III. This latter complex derives then directly from the  $\gamma$ -complex, not from II as an intermediate, but on the other hand, the III isomer evolved into II in acidic medium.

At pH < 3, I slowly evolved at room temperature into a mixture of II and another isomer (IV) characterized by 2-electron reduction waves at about -0.78 and -1.01 V. The relative amounts of II and III isomers depended on the acidity of the medium and the temperature, the proportion of II increasing with increasing temperature and pH. IV will be shown later to be the  $\beta(3,12)$ -isomer. The transformation of II into IV or conversely of IV into II has not been observed. We have not been able to obtain a pure crystalline sample of IV because the compounds always gave mixed crystals. Rather surprisingly, when the isomerization of the  $\gamma(1,2)\text{-[SiV}_2\text{W}_{10}\text{O}_{40}]^{6-}$  complex was carried out at pH 6.5 at the boiling temperature, a mixture of II and IV was obtained too. The interconversion between the different isomers is summarized in Scheme I.

**Infrared Characterization of the Four Isomers.** The IR spectra of the isomers are presented in Figure 3. The overall pattern

(8) (a) Pope, M. T.; Varga, G. M., Jr. *Inorg. Chem.* **1966**, *5*, 1249. (b) Altenau, J. J.; Pope, M. T.; Prados, R. A.; So, H. *Inorg. Chem.* **1975**, *14*, 417.

(9) Domaille, P. J.; Harlow, R. L. *J. Am. Chem. Soc.* **1986**, *108*, 2108.

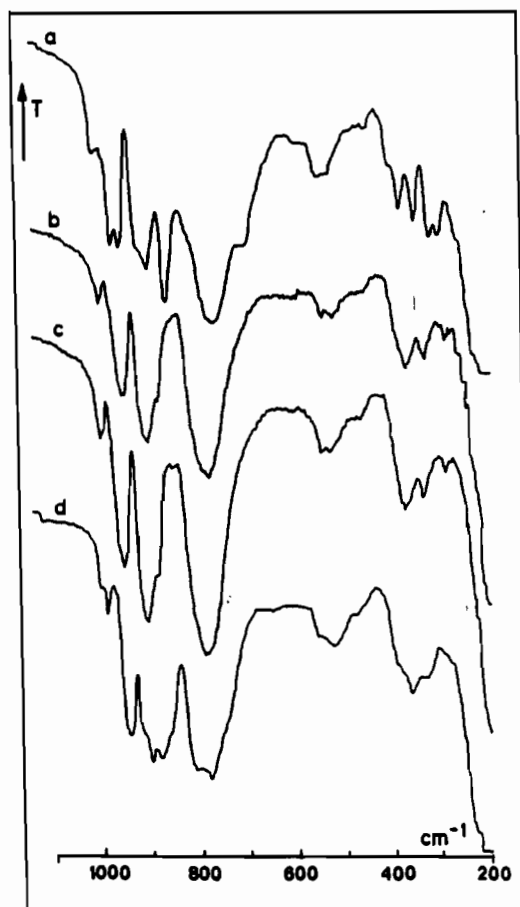


**Figure 3.** Infrared spectra of the cesium salts of the four  $[\text{SiV}_2\text{W}_{10}\text{O}_{40}]^{6-}$  anions as KBr pellets: (a)  $\gamma(1,2)$ -isomer; (b)  $\beta(8,12)$ -isomer; (c)  $\beta(3,12)$ -isomer with about 25% of  $\beta(8,12)$ -isomer purity; (d)  $\beta(3,8)$ -isomer.

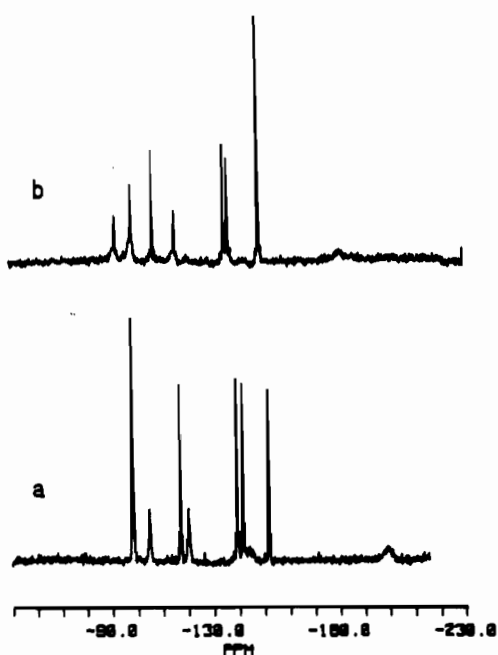


**Figure 4.**  $^{183}\text{W}$  NMR spectra of the  $\beta(8,12)$ - $[\text{SiV}_2\text{W}_{10}\text{O}_{40}]^{6-}$  (isomer II) anion: (a, lower spectrum) acidic form at  $\text{pH} \approx 0.6$ , 6578 scans, 20.8 MHz; (b, upper spectrum) deprotonated anion at  $\text{pH} \approx 6$ , 9036 scans, 10.4 MHz.

is consistent with complete dodecmetalate frameworks. It was previously mentioned that the low wavenumber region ( $400\text{--}300\text{ cm}^{-1}$ ) is the best one for the characterization of the geometrical isomers.<sup>10</sup> The five-band pattern observed for the  $\gamma$ -anion is in

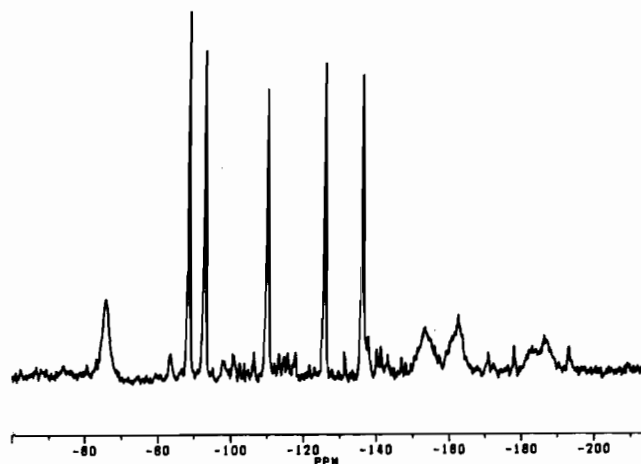


**Figure 5.** 20.8-MHz  $^{183}\text{W}$  NMR spectrum of the  $\beta(3,8)$ - $[\text{SiV}_2\text{W}_{10}\text{O}_{40}]^{6-}$  (isomer III) anion at  $\text{pH} \approx 7$ , 26 208 scans, 20.8 MHz.

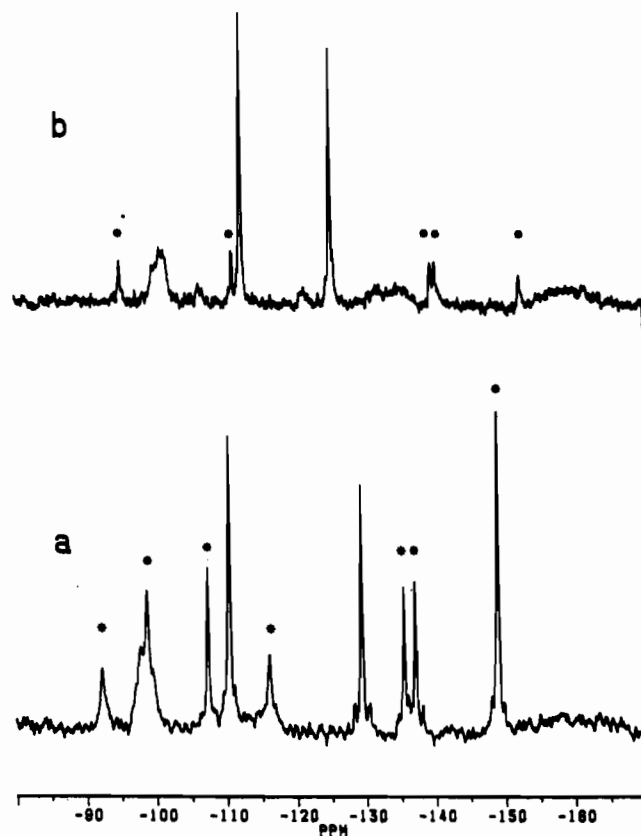


**Figure 6.**  $^{183}\text{W}$  NMR spectra of a mixture of the  $\beta(3,12)$  (isomer IV) and  $\beta(8,12)$  (isomer II)  $[\text{SiV}_2\text{W}_{10}\text{O}_{40}]^{6-}$  anions: (a, lower spectrum) deprotonated anion at  $\text{pH} 6$ , 9660 scans, 10.4 MHz, containing about 45% of IV and 55% of II; (b, upper spectrum) very acidic solution  $\text{pH} \ll 0$ , 3666 scans, 20.8 MHz, containing about 75% of IV and 25% of II. Asterisks show the  $^{183}\text{W}$  NMR lines arising from the  $\beta(8,12)$ -isomer in the mixture.

accordance with the low symmetry of the framework ( $C_{2v}$ ) and is very similar to that observed for the  $\gamma$ - $[\text{PV}_2\text{W}_{10}\text{O}_{40}]^{5-9}$  and the  $\gamma$ - $[\text{SiW}_{12}\text{O}_{40}]^{4-11}$  polyanions. A three-band pattern is observed for the other spectra, as generally observed for the  $\beta$ -framework,<sup>10</sup> that allows us to rule out a  $\gamma$ -framework for these three species.

**NMR Characterization of II–IV.** The analysis of the NMR spectra of the complexes is the best method to obtain information about their structures.

(10) Thouvenot, R.; Fournier, M.; Franck, R.; Rocchiccioli-Deltcheff, C. *Inorg. Chem.* 1984, 23, 598.

(11) Tézé, A.; Canny, J.; Thouvenot, R.; Hervé, G. To be submitted for publication.

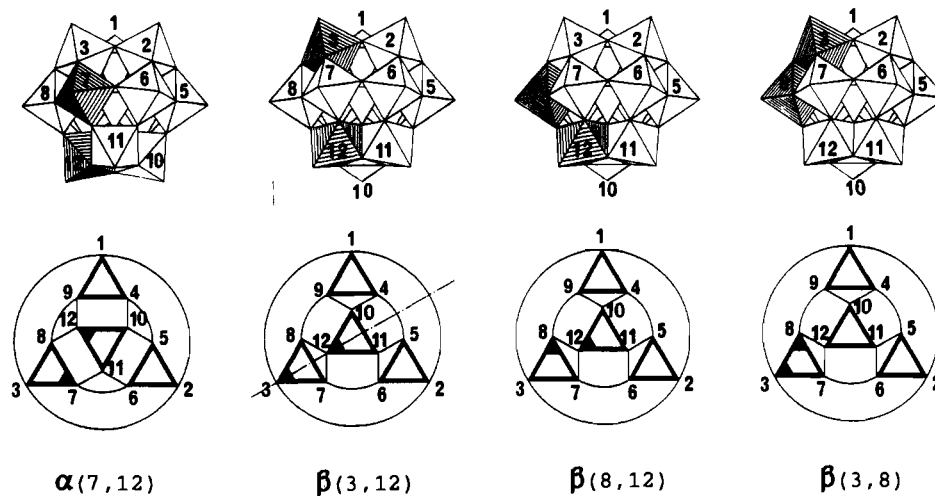


**Figure 7.** Polyhedral and schematic plane representations for the relevant  $\alpha$ - and  $\beta$ -[SiV<sub>2</sub>W<sub>10</sub>O<sub>40</sub>]<sup>6-</sup> isomers. In the plane representation, heavy and thin lines symbolize edge- and corner-sharing junctions respectively. The different atoms are numbered according to IUPAC recommendations.<sup>5b</sup> The vanadium atoms are symbolized by hatched octahedra and black triangles respectively.

**Anion II.** The <sup>29</sup>Si NMR spectrum shows a single line (−85.2 ppm) and the <sup>51</sup>V spectrum exhibit two poorly resolved lines at about −541 and −550 ppm for the deprotonated anion (pH 6, overall width about 800 Hz), consistent with two nonequivalent vanadium atoms. The <sup>51</sup>V NMR spectrum of the monoprotated form [HSiV<sub>2</sub>W<sub>10</sub>O<sub>40</sub>]<sup>5-</sup><sup>12</sup> shows only one signal at −548 ppm (pH 1;  $\Delta\nu_{1/2} = 250$  Hz). The <sup>183</sup>W NMR spectrum of the protonated complex shows 10 lines of equal integrated intensities (Figure 4a). Five are sharp ( $\Delta\nu_{1/2} \approx 1$  Hz; −98.3, −117.3, −139.5, −141.8, and −152 ppm), three have a width of about 20 Hz (−98.0, −104.9, and −120.5 ppm), and two are broad (−143 (150 Hz) and −200 ppm (80 Hz)). All lines are pH sensitive, but pH measurements in the concentrated and very acidic NMR solutions are not easy. The chemical shifts reported correspond to a solution of pH about 0.6.

The spectrum of the nonprotonated complex (pH 6, Figure 4b), consists of four sharp lines in the relative ratio 1:1:1:2 (−107.2, −135.6, −137, and −149 ppm) and four broad lines in the relative ratio 1:2:1:1 (−92, −98, −116, and −180 ppm). Such a spectrum is not consistent with any of the 40 divanadodecatungstosilicates based on  $\alpha$ -,  $\beta$ -, and  $\gamma$ -structures. The two lines of multiplicity 2 are then due to an accidental overlapping of lines of multiplicity 1.

**Anion III.** This complex (pH 7–8) shows a single <sup>29</sup>Si NMR line (−84.5 ppm) and two broad <sup>51</sup>V NMR lines (overall width 500 Hz) at about −521 and −518 ppm, consistent with two nonequivalent vanadium atoms. As for II, the <sup>183</sup>W NMR spectrum consists of 10 lines (Figure 5). Five of them are sharp (−90, −94, −111, −127, and −137 ppm) and five are broad (−67 (30 Hz)–153 (60 Hz), −161 (60 Hz), and −183 and −186 ppm (very broad)).

**Anion IV.** Since this isomer cannot be obtained in a pure form, the solutions investigated are always mixtures of II and IV isomers. Fortunately, the resonance lines of IV are well separated from those of the II, which allows to draw out the NMR parameters of the polyanion IV.

It shows a single <sup>29</sup>Si NMR line (−85.5 ppm) and two <sup>51</sup>V NMR lines at −541 and −547 ppm, consistent with two nonequivalent vanadium atoms. The <sup>183</sup>W NMR spectrum (pH 6) (Figure 6a), consists of five lines of equal intensity. Two of them are sharp: −110.3 ( $\Delta\nu_{1/2} = 1$  Hz;  $^2J_{W-W} = 4.9$  and 15.6 Hz), −129.3 ppm ( $\Delta\nu_{1/2} = 1$  Hz;  $^2J_{W-W} = 4.9, 6.4, 19.8,$  and 24.3 Hz). Among the three others, one is broad (−100 ppm (about 20 Hz)) and the two others are very broad (−130 and −160 ppm (more than 100 Hz)). An analogous spectrum is observed in acid solution (Figure 6b).

**Structures of the Three Isomers.** Considering only the  $\alpha$ - and

$\beta$ -structures of the 12-tungstoheteropolyanions, according to the IR characteristics, there are 19 geometrical isomers for the [SiV<sub>2</sub>W<sub>10</sub>O<sub>40</sub>]<sup>6-</sup> complex. II and III give five sharp lines in their <sup>183</sup>W NMR spectrum, which is consistent only with two  $\beta$ -[SiV<sub>2</sub>W<sub>10</sub>O<sub>40</sub>]<sup>6-</sup> structural possibilities (Figure 7). An unambiguous choice between them would require the observation of all the  $^2J_{W-W}$  coupling constants, which is not feasible here because of limited *S/N* and broad lines. However, we can consider the width of the broad lines. For the  $\beta(8,12)$ -isomer, three relatively sharp lines (edge V–W coupling for W(3), W(10), and W(11)) and two broad lines (corner V–W coupling for W(7) and W(9)) are expected. For the  $\beta(3,8)$ -isomer, all but one of the lines are expected to be very broad (only a V–W edge coupling for W(7)). Comparison with the experimental data leads us to propose an assignment of the  $\beta(8,12)$ -structure to II and of the  $\beta(3,8)$ -structure to III.

Additional support for this assignment comes from the positions of the broad lines:<sup>13</sup> the four broad resonances of III appear at high field and should be the four corner-coupled W(1), W(2), W(9), and W(12) tungsten atoms of the  $\beta(3,8)$ -isomer. Moreover, its relatively sharp line appears at high frequency and corresponds to W(7) edge-coupled to both vanadium atoms. For II, the high-field resonance corresponds to the W(9) tungsten (only corner-coupled to vanadium) of the  $\beta(8,12)$ -isomer, and the broadest line (W(7) simultaneously edge- and corner-coupled) falls consistently in the middle of the spectrum (Figure 4a).

The isomer IV has necessarily a binary symmetry element since its <sup>183</sup>W NMR spectrum shows only two sharp lines. Two structures can be considered (Figure 7): one is the  $\beta(3,12)$ -structure, with a symmetry plane containing the two nonequivalent nonadjacent vanadium atoms; the other is the  $\alpha(7,12)$ -structure with a binary symmetry axis exchanging the vanadium atoms. The  $\alpha$ -structure can be ruled out because only one <sup>51</sup>V resonance should be observed. On the contrary, two <sup>51</sup>V lines are expected for the  $\beta(3,12)$ -structure, as actually observed. Moreover, in the  $\alpha$ -structure, the two sharp <sup>183</sup>W NMR lines (W(1) equivalent to W(5) and W(2) equivalent to W(4), respectively) would have the same satellite pattern with a mutual corner coupling constant of about 15 Hz or more, which was not actually observed. Therefore, isomer IV has the  $\beta(3,12)$ -structure. Among the two sharpest lines, the resonance at −110.3 ppm, with only one  $^2J_{W-W}$  corner coupling, is assigned to the W(4)–W(5) atoms, and the resonance

(12) The *pK* value for  $\beta(8,12)$ -[HSiV<sub>2</sub>W<sub>10</sub>O<sub>40</sub>]<sup>5-</sup> is 3.2; therefore, this polyanion is present in its protonated form at pH 1.

(13) Tungsten atoms that edge share a lower oxidation state metal (V, Ti, Pb) consistently fall at higher frequencies while corner sharing results in low-frequency shifts. Double edge sharing enhances this effect while simultaneous edge–corner sharing results in an intermediate resonance frequency: Domaille, P. J.; Knoth, W. H. *Inorg. Chem.* **1983**, *22*, 818; see also ref 7. We acknowledge a reviewer for suggesting the use of this supplementary argument for the structural discussion.

at -129.3 ppm, with two pairs of satellites corresponding to  $^2J_{W-W}$  corner coupling is assigned to the W(6)-W(9) atoms. Because of its relative sharpness ( $\Delta\nu_{1/2} = 20$  Hz) and of its high frequency<sup>13</sup> the line at -100 ppm arises from the equivalent W(10)-W(11) atoms only edge coupled to vanadium. The two very broad low frequency resonances are from the W(1)-W(2) and W(7)-W(8) pairs, which are both corner-coupled with vanadium atoms. Precise assignment of these lines cannot be proposed on the basis of the present data.

### Conclusion

This study establishes that the nature of the isomerization products of the  $\gamma(1,2)$ -[SiV<sub>2</sub>W<sub>10</sub>O<sub>40</sub>]<sup>6-</sup> polyanion is strongly dependent on the experimental conditions, especially on the pH of the aqueous solution. Since the  $\gamma$ -isomer is stable in nonaqueous solution, the isomerization proceeds via hydrolytic cleavage of W-O or/and V-O bonds. In all cases,  $\beta$ -[SiV<sub>2</sub>W<sub>10</sub>O<sub>40</sub>]<sup>6-</sup> isomers were

obtained and appear then to be more resistant to hydrolysis, in basic as well as in acid solution, than the  $\gamma$ -structure, which is characterized by a bis( $\mu$ -oxo) bond between the vanadium atoms.

We are not able to derive precisely the mechanism of this hydrolytic reaction, but it appears to depend strongly on the nature, number, and protonation state of the oxo bridges between the metallic atoms concerned by the reaction. For example, a protonated form of the  $\gamma$ -complex is easily obtained in acid solution and evolves mainly to the  $\beta(3,12)$ -isomer. On the contrary, the unprotonated complex  $\gamma(1,2)$ -[SiV<sub>2</sub>W<sub>10</sub>O<sub>40</sub>]<sup>6-</sup> appears to be stable (or very kinetically inert) in solution ( $3 < \text{pH} < 5$ ). At higher pH, there are probably selective cleavages of V-O-V or/and V-O-W bonds, leading to unstable species that rearrange to give the more stable  $\beta$ -complexes.

**Acknowledgment.** We are grateful to a reviewer for suggesting the incorporation of Scheme I, which summarizes the interconversion processes.

Contribution from the Anorganisch-Chemisches Institut, Westfälische Wilhelms-Universität Münster, Wilhelm Klemm Strasse 8, D-4400 Münster, Federal Republic of Germany, Spectrochimie du Solide, Université Pierre et Marie Curie, 4 Place Jussieu, 75252 Paris Cedex 05, France, Systemes Energetiques et Transferts Thermiques, Université de Provence, Centre de Saint-Jerôme, Case 152, Avenue Escadrille Normandie-Niemen, 13397 Marseille Cedex 13, France, and Molten Salts Group, Chemistry Department A, Building 207, The Technical University of Denmark, DK-2800 Lyngby, Denmark

## Crystallographic and <sup>27</sup>Al NMR Study on Premelting Phenomena in Crystals of Sodium Tetrachloroaluminate

Bernt Krebs,<sup>†</sup> Horst Greiwing,<sup>†</sup> Claus Brendel,<sup>†</sup> Francis Taulelle,<sup>‡</sup> Marcelle Gaune-Escard,<sup>§</sup> and Rolf W. Berg<sup>\*||</sup>

Received May 14, 1990

The crystal structure of NaAlCl<sub>4</sub> was determined in the orthorhombic space group  $P2_12_12_1$  ( $D_2^7$ , No. 19;  $Z = 4$ ) at temperatures 138, 150, and  $154 \pm 0.2$  °C, resulting in the lattice parameters  $a = 10.442$  (4), 10.449 (3), 10.455 (2) Å,  $b = 9.973$  (3), 9.993 (2), 10.002 (2) Å, and  $c = 6.202$  (2), 6.206 (2), 6.204 (2) Å, respectively. Samples of the compound were investigated by differential scanning calorimetry. <sup>27</sup>Al NMR spectra were obtained on NaAlCl<sub>4</sub> and LiAlCl<sub>4</sub> solids as a function of temperature up to and above the melting points, at 157 and 146 °C, respectively. In accordance with the enhanced premelting heat contents, the observed phenomena indicate the existence of a specific dynamical behavior of the components in the two crystals, involving reorientational noncontinuous movements of the AlCl<sub>4</sub><sup>-</sup> ions and translational jumps of the alkali-metal cations.

### Introduction

In a study<sup>1</sup> of the phase diagram of the NaCl-AlCl<sub>3</sub> system, the enthalpy of melting was determined cryoscopically to be about 15.5 kJ mol<sup>-1</sup>. However, much higher values have been obtained calorimetrically: Rogers<sup>2</sup> found  $19.4 \pm 0.4$  kJ mol<sup>-1</sup>, and Denielou et al.<sup>3</sup> found  $20.3 \pm 0.5$  kJ mol<sup>-1</sup>. Also, in an impressive paper, Dewing<sup>4</sup> reported the enthalpy of liquid NaAlCl<sub>4</sub> versus temperature and obtained a  $\Delta H_f$  value of 18.4 kJ mol<sup>-1</sup>. These calorimetric values are so close that they are probably correct within  $\pm 2.0$  kJ mol<sup>-1</sup>. Due to the internal consistency, according to Dewing,<sup>4</sup> no serious error should exist in any of his final thermodynamic quantities (including  $\Delta H_f$ ).

The apparent disagreement between the values determined by cryoscopy and calorimetry has been considered<sup>1</sup> to be due to a possible structural change (premelting) in NaAlCl<sub>4</sub>, around 140-150 °C. Upon heating (see Figure 1), the experimental enthalpy content of solid NaAlCl<sub>4</sub> follows a linear trend up to a temperature  $T_p$  of around 137 °C, from which temperature it starts to deviate positively. Apparently, the solid absorbs excessive heat of  $\Delta H_p = \text{ca. } 4.5$  kJ mol<sup>-1</sup> until finally, at the melting point ( $T_f = \text{ca. } 156.7$  °C), it absorbs the cryoscopically determined heat of ca. 15.5 kJ mol<sup>-1</sup>.

Table I. Crystallographic Data for Sodium Aluminum Chloride

chem formula:	NaAlCl <sub>4</sub>
$a$	$10.442$ (4), $10.449$ (3), $10.455$ (2) Å
$b$	$9.973$ (3), $9.993$ (2), $10.002$ (2) Å
$c$	$6.202$ (2), $6.206$ (2), $6.204$ (2) Å
$\alpha = \beta = \gamma$	$90^\circ$
$V$	$645.9$ , $648.0$ , $648.8$ Å <sup>3</sup>
$Z$	4
$\rho_{\text{calcd}}$	$1.972$ , $1.966$ , $1.963$ g cm <sup>-3</sup>
fw	191.78
space group:	$P2_12_12_1$ ( $D_2^7$ ) (No. 19)
$T$	138, 150, 154 °C
$\lambda(\text{Mo K}\alpha)$	$0.71069$ Å
$\mu$	$18.8$ cm <sup>-1</sup>
abs cor:	none
$R(F_o)$	$0.0350$ , $0.0442$ , $0.0476$
$R_w(F_o^2)$	$0.0342$ , $0.0425$ , $0.0403$

To study this assumed premelting effect, we have now determined the structure of NaAlCl<sub>4</sub> single crystals by means of X-ray diffraction, just below the melting point. Previously, the structure has been solved at ambient temperatures<sup>5-8</sup> and at 125 °C.<sup>9</sup> Also,

<sup>†</sup> Westfälische Wilhelms-Universität Münster.

<sup>‡</sup> Université Pierre et Marie Curie.

<sup>§</sup> Université de Provence.

<sup>||</sup> The Technical University of Denmark.

- (1) Berg, R. W.; Hjulær, H. A.; Bjerrum, N. J. *Inorg. Chem.* **1984**, *23*, 557.
- (2) Rogers, L. J. *J. Chem. Thermodyn.* **1980**, *12*, 51.
- (3) Denielou, L.; Petitet, J.-P.; Tequi, C. *J. Chem. Eng. Data* **1982**, *27*, 129.
- (4) Dewing, E. W. *Metall. Trans. B* **1981**, *12B*, 705.
- (5) Baenziger, N. C. *Acta Crystallogr.* **1951**, *4*, 216.
- (6) Scheinert, W.; Weiss, A. *Z. Naturforsch., A* **1976**, *31A*, 1354.